Journal of Medicinal Chemistry

Article

pubs.acs.org/jmc

Structure–Activity Relationship of Imidazopyridinium Analogues as Antagonists of Neuropeptide S Receptor

Samarjit Patnaik,[†] Juan J. Marugan,*[,†] Ke Liu,[†] Wei Zheng,[†] Noel Southall,[†] Seameen J. Dehdashti,[†] Annika Thorsell,[‡] Markus Heilig,[‡] Lauren Bell,[‡] Michelle Zook,[‡] Bob Eskay,[‡] Kyle R. Brimacombe,[†] and Christopher P. Austin[†]

[†]National Center for Advancing Translational Sciences, National Institutes of Health, 9800 Medical Center Drive, Rockville, Maryland 20850, United States.

[‡]National Institute on Alcohol Abuse and Alcoholism, National Institutes of Health, Bethesda, Maryland 20892, United States

Supporting Information

ABSTRACT: The discovery and characterization of a novel chemical series of phosphorothioyl-containing imidazopyridines as potent neuropeptide S receptor antagonists is presented. The synthesis of analogues and their structure–activity relationship with respect to the Gq, Gs, and ERK pathways is detailed. The pharmacokinetics and in vivo efficacy of a potent analogue in a food intake rodent model are also included, underscoring its potential therapeutic value for the treatment of sleep, anxiety, and addiction disorders.

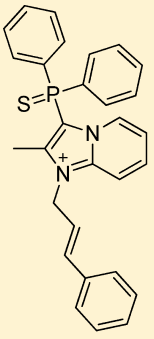

20e

Ca^{2+} IC_{50} = 9.6 nM
cAMP IC_{50} = 45 nM
ERK IC_{50} = 1.3 nM
[^{125}I]NPS IC_{50} = 3.5 nM

INTRODUCTION

Neuropeptides are short chains of amino acids or small proteins that play a crucial role in controlling intracellular neuronal signaling. They bind to cell-surface receptors and elicit a variety of physiological responses.[1] The 21-amino acid neuropeptide S (NPS), named "S" because of a conserved N-terminus serine residue found across vertebrate species, has received considerable attention in the recent past. The cognate receptor for NPS, neuropeptide S receptor (NPSR), was first described by Sato in 2002, but the endogenous peptide was left uncharacterized.[2] The Reinscheid group deorphanized the receptor and also identified regions of the brain where the peptide and its receptor are expressed.[3] They also detailed the pharmacology of the NPS/NPSR system using Chinese hamster ovary (CHO) and human embryonic kidney 293 (HEK 293) cells stably expressing human and murine variants of NPSR. NPS acted as an agonist in these cell lines, causing a dose-dependent increase in the levels of intracellular calcium, cyclic adenosine monophosphate (cAMP), and p42/p44 mitogen-activated protein kinase (MAPK) phosphorylation. This suggested that NPSR is coupled to the Gq and Gs proteins and the MAPK pathway, respectively. Furthermore, they synthesized the human [^{125}I]Tyr10-hNPS radiolabeled peptide and showed it to be an agonist that is equipotent to the natural ligand NPS and can be used in radiolabeled ligand displacement assays.[4] The pharmacological characterization was extended to an Asn107Ile mutant and a C-terminal splice variant that were linked to asthma.[5,6]

Leading in vivo studies published by Xu et al.[3] showed an increase in locomotor activity and reduction of all stages of sleep upon supraspinal administration of NPS in mice. Paradoxically, they also demonstrated a reduction in anxiety in four different validated mouse models of anxiety, earning NPS the unique distinction of being a novel activating anxiolytic.[7] Experiments with Long–Evans rats also showed that administration of NPS in the lateral brain ventricle leads to anorexia-like symptoms with suppression of food intake.[8] Ciccocioppo and co-workers reported that administration of NPS in the lateral hypothalamus of the rat brain resulted in a significant increase in cue-induced alcohol-seeking behavior in an alcohol relapse rat model.[9] This effect was reduced by the selective oxerin receptor antagonist SB-334867,[10] indicating the presence of a strong link between the hypocretin1/orexinA and NPS signaling pathways. Similar in vivo work has also implicated this circuitry's relevance toward addiction to cocaine and morphine.[11] The types of physiological changes observed in various rodent models after central administration of NPS have been summarized in several reviews.[12]

Systematic exploration of the amino acids along the SFRNGVGTGMKKTSFQRAKS peptide sequence of NPS has not only identified key residues essential for agonist activity but also led to the discovery of novel peptide antagonists.[13] Recently several small-molecule antagonists of

Received: June 19, 2013

dx.doi.org/10.1021/jm400904m | J. Med. Chem. XXXX, XXX, XXX–XXX

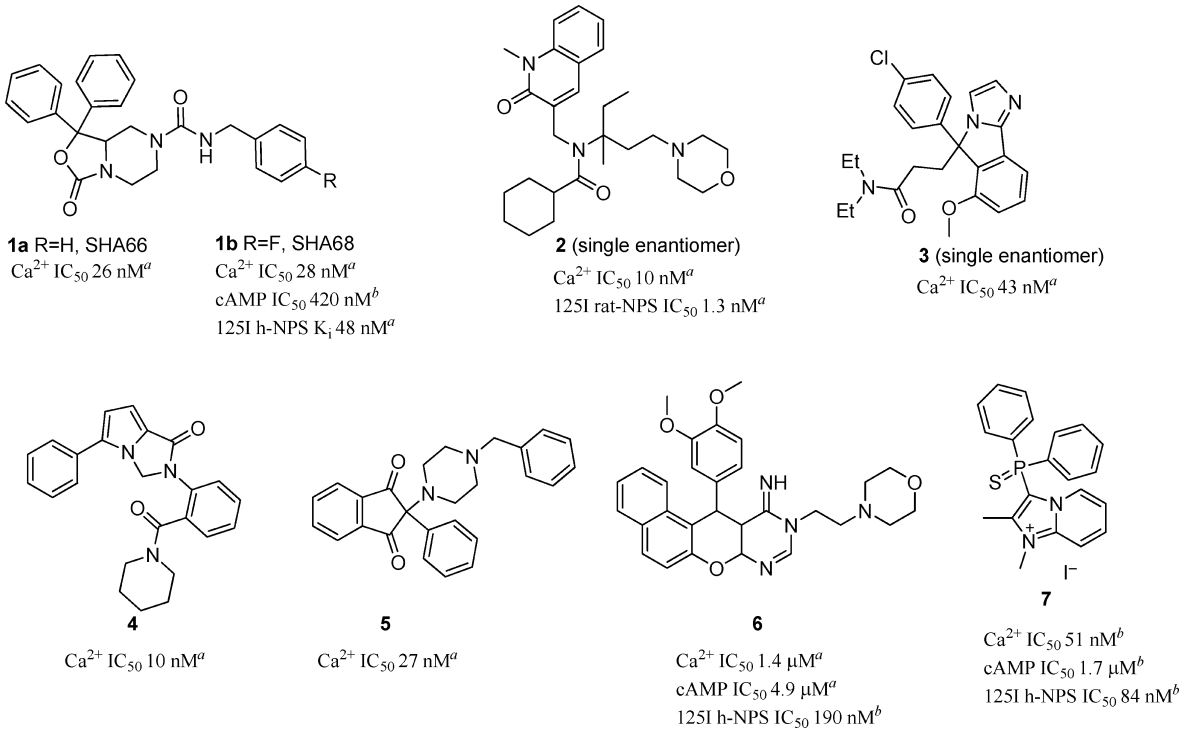

Figure 1. Potent small-molecule antagonists of the NPSR pathway. [a]Activity described in the literature. [b]Activity determined in house.

Scheme 1. Synthetic Scheme for the Screening Hit and Analogues[a]

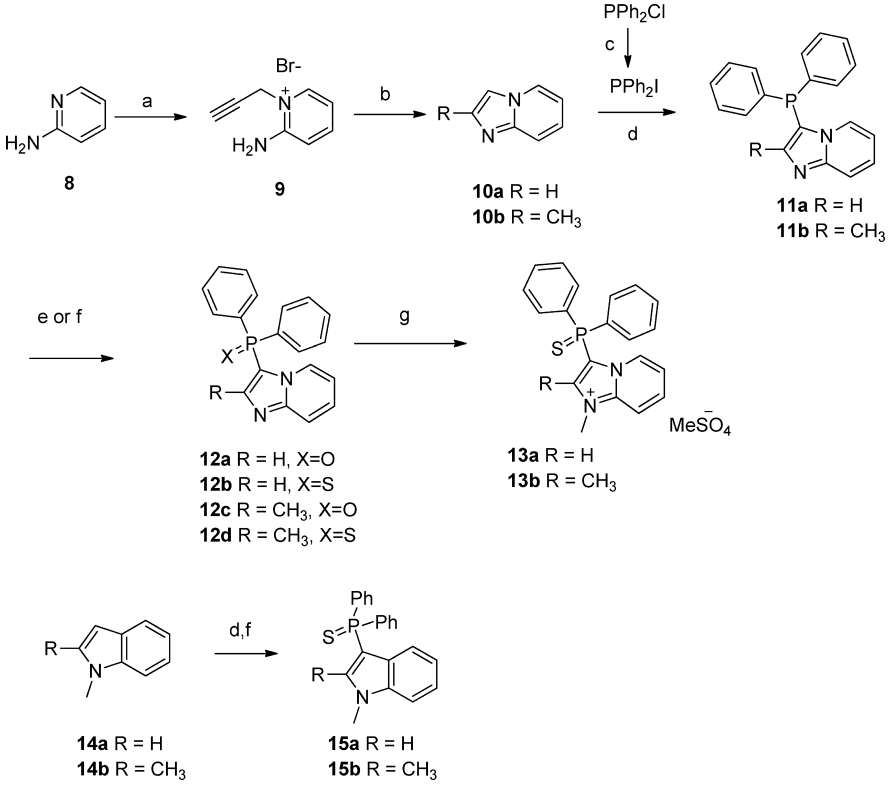

[a]Reagents and conditions. (a) EtOH, $CHCCH_2Br$, reflux, 47% yield; (b) $Pd(PPh_3)_4$, CuI, DMF, rt, 72% yield; (c) TMSI, toluene; (d) py, Et_3N, PPh_2I; (e) 30% H_2O_2, 30−50% yield over two steps; (f) sulfur, 30−50% yield over two steps; (g) Me_2SO_4, 1,4-dioxane, sealed tube, 100−120 °C, 30−50% yield.

the NPS/NPSR pathway have also been reported in the literature. This has been a promising development, as these molecules serve not only as vital tools for understanding pharmacology but also hold potential for drug development toward anxiety, food, and addiction disorders. In this regard, two molecules disclosed by Takeda Pharmaceuticals,[14] SHA66

dx.doi.org/10.1021/jm400904m | J. Med. Chem. XXXX, XXX, XXX−XXX

Scheme 2. Synthetic Scheme toward Tertiary Alcohols 19a and 19b[a]

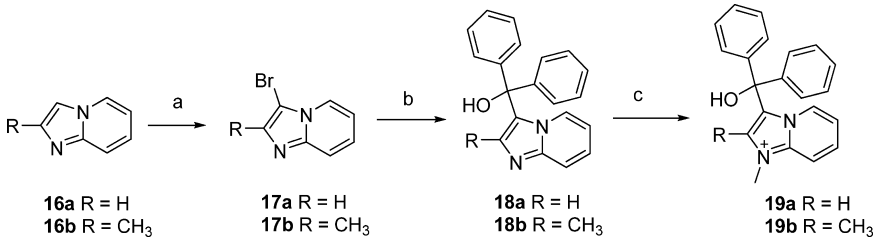

[a]Reagents and conditions. (a) NBS; (b) iPrMgCl·LiCl, THF, Ph_2CO, 18% yield for **18a** and 31% yield for **18b**; (c) Me_2SO_4, 1,4-dioxane, sealed tube, 100−120 °C, 50−60% yield.

Table 1. SAR of Initial Analogues: The cAMP and Ca^{2+} Assay Activities Are Mean IC_{50} Values with Standard Deviations (SDs) from Two Separate Experiments, Each Run in Duplicate; The ERK Assay Activities Are Mean IC_{50} Values with SDs from One Experiment Run in Duplicate

#	Structure	R	cAMP IC_{50} μM	Ca^{2+} IC_{50} μM	ERK IC_{50} μM
11a	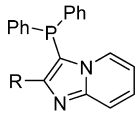	H	Inact	35[a]	<50%[b]
12a	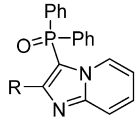	H	Inact	Inact	<50%[b]
12c		Me	Inact	27 ± 13[a]	<50%[b]
12b	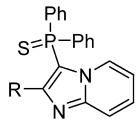	H	63 ± 0[a]	4.03 ± 0.07	<50%[b]
12d		Me	18 ± 3	1.0 ± 0.16	0.0091, 0.030[c]
13a	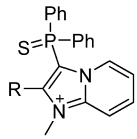	H	39 ± 0[a]	2.5 ± 0.4	<50%[b]
7		Me	1.7 ± 0.1	0.051 ± 0.008	0.030 ± 0.006
15a	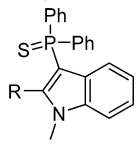	H	Inact	7.3± 2.3	<50%[b]
15b		Me	Inact	2.8 ± 0.0	<50%[b]
18a	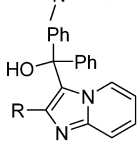	H	Inact	Inact	<50%[b]
18b		Me	Inact	Inact	<50%[b]
19a	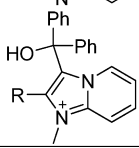	H	Inact	Inact	<50%[b]
19b		Me	Inact	Inact	<50%[b]

"Inact" = inactive. [a]This compound showed partial efficacy in its antagonistic behavior. [b]This compound showed <50% inhibition at the highest concentration (50 μM) tested. [c]Both IC_{50} values are reported here, as we consider the standard deviation between the replicates to be significant.

(**1a**) and SHA68 (**1b**) (Figure 1), have been characterized extensively as potent inhibitors of the NPS/NPSR signaling pathway. A 50 mg per kilogram (mpk) intraperitoneal (IP) dose of **1b** was also able to reduce NPS-induced hyperlocomotion by about 50% in a 90 min mouse model.[15] Reported pharmacokinetic (PK) studies showed brain levels of ∼6 μM at 15 min and ∼2 μM at 2 h, which are well beyond its in vitro half-maximal inhibitory concentration (IC_{50}). Moreover, the bioactive enantiomer of **1b** has recently been identified.[16] Merck has disclosed potent inhibitors from two separate chemical series (**2** and **3**).[17,18] The best compound from a series of quinolinones, **2**, demonstrated high ex vivo occupancy of NPSR in discrete regions of the rat brain after a 30 mpk IP dose. GSK and Actelion Pharmaceutical Ltd. have also reported novel NPSR antagonists around the scaffolds represented by pyrroloimidazolone (**4**) and indanone (**5**), respectively.[19,20] Our efforts within the NIH have resulted in the disclosure of a naphthapyranopyrimidine probe (**6**), where

dx.doi.org/10.1021/jm400904m | J. Med. Chem. XXXX, XXX, XXX−XXX

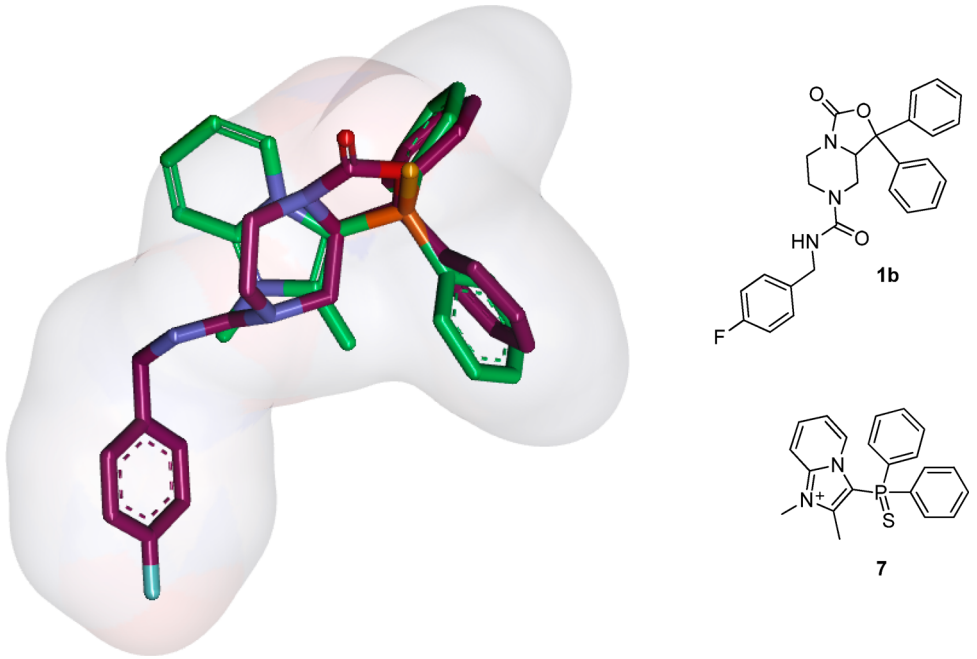

Figure 2. Overlap model of **1b** and screening hit **7** (green).

structural changes in the same chemical series led to the discovery of selective modulators of either the Gq or Gs pathway.[21] Dal Ben has summarized the structure–activity relationship (SAR) around these small NPSR antagonists in a recent review.[22] Herein we disclose the discovery of another structurally uncommon chemotype that after medicinal chemistry optimization produced a compound with potent antagonism of the NPS/NPSR signaling pathway.

RESULTS AND DISCUSSION

Our efforts to discover novel antagonists for the NPS pathway started with the development of a high-throughput homogeneous time-resolved fluorescence (HTRF) assay that could measure the formation of cAMP upon binding of NPS to NPSR using CHO cells stably expressing NPSR. This cAMP assay was used to screen 222 256 compounds in the quantitative high-throughput screening (qHTS) format.[23] This effort led to the discovery of the inhibitor 3-(diphenylphosphorothioyl)-1,2-dimethylimidazo[1,2-*a*]pyridin-1-ium iodide (**7**) (Figure 1).[24] The antagonistic activity of this compound was further confirmed in orthogonal assays measuring the reduction of calcium mobilization in the same cell line and in a radiolabeled NPS displacement assay. The unusual functionality within the molecule prompted us to evaluate its stability in various aqueous buffers. We found that **7** did not decompose into any other species after exposure to Hank's balanced buffer solution (HBBS) or phosphate-buffered saline (PBS) over a period of 48 h. This confirmed its robust chemical stability and spurred a medicinal chemistry effort aimed at examining the key structural elements that are necessary for the antagonistic activity. In the previous chemotype reported by us (**6**),[20] we observed a structure-related differential in the antagonist activities toward the Gs and Gq pathways within the same NPS antagonistic series.[20] At the present moment, it is not clear which signaling pathways are linked to different biological responses observed by NPSR activation. Therefore, we decided to examine and report here the inhibition of both the Gs and Gq pathways with the cAMP and Ca^{2+} assays, respectively. In addition, we also analyzed the inhibition of ERK activation, as the NPSR is also coupled to the MAPK pathway. To that end, the synthetic route shown in Scheme 1 was developed for our SAR exploration. While the desmethyl compound **10a** was commercially available, 2-methylimidazo[1,2-*a*]pyridine (**10b**) could be accessed via a known palladium-catalyzed internal cyclization of the amino group on the pendant alkyne in 2-amino-1-(propargyl)pyridinium bromide (**9**).[25] The Tolmachev protocol allowed for the electrophilic aromatic substitution at the 3-position for the introduction of the diphenylphosphino group.[26] While **10a** could be reacted with chlorodiphenylphosphine, the 2-methyl counterpart **10b** required the use of the more reactive iododiphenylphosphine, which was generated from chlorodiphenylphosphine and trimethylsilyl iodide.[27] Treatment of crude phosphines **11a** and **11b** with either elemental sulfur or hydrogen peroxide provided the diphenylphosphorothioyl species **12b** and **12d** or the diphenylphosphoryl species **12a** and **12c**, respectively. A final alkylation of **12b** and **12d** with dimethyl sulfate led to imidazopyridinium salts **13a** and **13b**, respectively.[28] These imidazopyridinium salts could be purified by normal or reversed-phase chromatographic techniques, and the nature of the counteranion proved to be inconsequential toward the bioactivity. The generation of the indole variants **15a** and **15b** were carried out in similar fashion from commercially available **14a** and **14b**, respectively.[29]

We were also interested in evaluating a tertiary diphenyl alcohol group as a possible bioisosteric replacement for the phosphorothioyl group. To that end, the 3-bromoimidazopyridines **17a** and **17b** were generated from **16a** and **16b**, respectively, with *N*-bromosuccinimide (NBS) (Scheme 2). Subsequent halogen–metal exchange using the chemistry described by Krasovskiy and Knochel[30] was followed by addition of benzophenone to generate the corresponding tertiary alcohols **18a** and **18b**. These alcohols could be chemoselectively alkylated at N1 in dioxane to yield analogues **19a** and **19b**, respectively.

dx.doi.org/10.1021/jm400904m | *J. Med. Chem.* XXXX, XXX, XXX–XXX

As an initial confirmation of our HTS data, we obtained IC_{50}'s similar to our previous values in both assays for our resynthesized original hit compound **7**. In addition, the activity data in Table 1 indicate the sensitivity of the 2-methylimidazopyridine core and the phosphorothioyl moieties toward structural change. Thus, elimination of the 2-methyl substituent reduced the activity 3−25-fold (e.g., **12b** vs **12d** and **13a** vs **13b**) in the cAMP assay. Replacement of the sulfur atom in the thiophosphoryl functional group by an oxygen (**12c** vs **12d**) or its elimination (**11a**) abolished the antagonist activity. Similarly, diphenyl alcohols **18a** and **18b** and their corresponding N1-methylated analogues **19a** and **19b** were inactive. The indole Replacement of the imidazopyridinium core with indole in **15a** and **15b** also proved deleterious toward the activity. In general, the active compounds appeared to have enhanced potencies in the Ca^{2+} and ERK assays.[31]

The activity results of the first set of synthetic compounds (Table 1) convinced us to preserve the 2-methylimidazopyridinium core and the thiophosphorus moiety in our subsequent analogue design. The striking structural similarity between the diphenylphospho group in our screening hit and the geminal diphenyl group in **1a** and **1b** prompted us to consider simple overlap models between these compounds (Figure 2). Moreover, in-house [^{125}I]Tyr10-NPS displacement experiments had disclosed that both chemical series are able to compete with the natural ligand, and therefore, we hypothesized that both orthosteric antagonists would bind to the same region, probably with similar three-dimensional geometry. When we overlapped the geminal diphenyl substituents, we realized that the oxazolidinone dipole aligned well with the phosphorothioyl moiety. The piperidine in **1b** also overlapped reasonably with the imidazole of the imidazopyridine. However, it seemed that we were probably missing a hydrophobic phenyl ring at the lower portion of our compound which may have been the critical element in the higher potency of **1a** and **1b**. Fortunately, we were able to test this hypothesis by utilizing the chemistry that had been developed to resynthesize screening hit **7**. To that end, **12d** would be an ideal intermediate for alkylation at N1 with various commercially available bromides that would place a phenyl ring different numbers of spacer units away from the core of the molecule (Scheme 3).

Scheme 3. Synthetic Route to Analogues with Chemical Diversity at Position 1

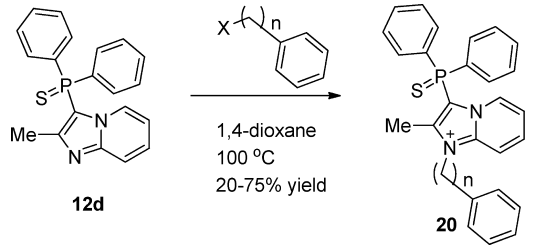

Table 2 summarizes the activities of the analogues generated to test our hypothesis. Compound **20a** with a phenyl ring one methylene unit away from N1 had similar potency as the original hit **7**. This also held true for **20b** and **20c** with ethylene and ethanone spacer units, respectively, between the phenyl ring and N1. Remarkably, compound **20d** with the phenylpropyl chain recorded substantial improvements in potency (IC_{50} = 110, 1, and 2 nM in the cAMP, calcium, and ERK assays, respectively). The same trend was observed for **20e** with

Table 2. SAR of Analogues at Position 1: The cAMP and Ca^{2+} Assay Activities Are Mean IC_{50} Values with SDs from Two Separate Experiments, Each Run in Duplicate; The ERK Assay Activities Are Mean IC_{50} Values with SDs from One Experiment Run in Duplicate

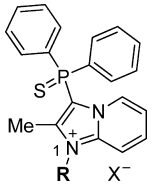

R	#	cAMP IC_{50} μM	Ca^{2+} IC_{50} μM	ERK IC_{50} μM
	7	1.7 ± 0.1	0.051 ± 0.008	0.030 ± 0.006
	20a	1.3 ± 0.0	0.032 ± 0.005	0.016 ± 0.001
	20b	2.1 ± 0.2	0.073 ± 0.023	0.016, 0.063[b]
	20c	2.1 ± 0.0	0.080 ± 0.013	0.013, 0.028[b]
	20d	0.11 ± 0.01	0.0016, <0.0005[a]	0.0035, <0.0005[a]
	20e	0.045 ± 0.000	0.00096 ± 0.00023	0.0013 ± 0.0007
	20f	0.94 ± 0.08	0.0011, < 0.0005[a]	0.015 ± 0.000
	20g	0.71 ± 0.00	0.013 ± 0.002	0.0062 ± 0.0007

[a]The two replicate IC_{50} values are reported here, one (<0.5 nM) being less than could be detemined accurately by the assay. [b]Both IC_{50} values are reported here, as we consider the standard deviation between the replicates to be significant.

the more constrained propenylbenzene appendage, which recorded a benchmark potency of 45 nM in the cAMP assay. Spacing the phenyl ring by four (**20f**) or five (**20g**) methylene units led to erosion of the potent activity achieved with three spacer units. Each analogue in Table 2 showed at least a 25-fold drop in its potency in the cAMP assay compared with its individual potency in the calcium or ERK assay. At this juncture, we also evaluated additional substitution in the phenyl ring when it was optimally separated from N1 of the imidazopyridine core by a propenyl group. Table 3 displays the activities of such compounds in the context of the Gs and Gq pathways. Although many types of substitutions were tolerated, unsubstituted **20e** remained the most potent compound. It appeared that meta substitution was slightly less tolerated than para substitution, as exemplified by compounds **21g** and **21c** versus **21f** and **21d**, respectively. The weakest inhibitor in this series was the 2-naphthyl-substituted compound **21i**, indicating a size restriction that might be associated with the hydrophobic region that accommodates the phenyl group in **20e**.

While we had discovered potent antagonists of the NPS/NPSR signaling pathway, it was crucial to compare the activities of this structural class with those of the best-in-class small-molecule inhibitors in the literature. We did this in the context of our functional assays as well the radiolabeled binding assay (Table 4). We observed that **20e** was 5-fold more potent than **1b** in the calcium and displacement assays and 9-fold more potent in the cAMP assay. On the other hand, the potencies in these assays were comparable to those of the active enantiomer of **2** reported by Merck. Comopound **20e** appeared to be a more potent inhibitor of ERK phosphorylation. We also decided to compare the intrinsic stabilities of these key NPSR

dx.doi.org/10.1021/jm400904m | J. Med. Chem. XXXX, XXX, XXX−XXX

Table 3. SAR of the Substituted Phenyl Ring: The cAMP and Ca^{2+} Assay Activities Are Mean IC_{50} Values with SDs from Two Separate Experiments, Each Run in Duplicate

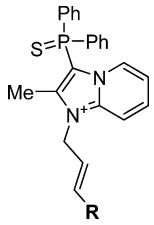

#	R	cAMP IC_{50} (μM)	Ca^{2+} IC_{50} (μM)
20e		0.044 ± 0.000	0.00096 ± 0.00023
21a	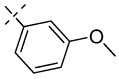	0.11 ± 0.00	0.0032 ± 0.0005
21b		0.094 ± 0.008	0.0034 ± 0.0016
21c	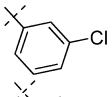	0.22 ± 0.00	0.0092 ± 0.0029
21d	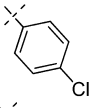	0.12 ± 0.01	0.0022, 0.0071[a]
21e	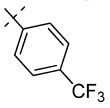	0.40 ± 0.00	0.013, 0.0045[a]
21f	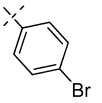	0.17 ± 0.01	0.0057 ± 0.0000
21g	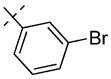	0.67 ± 0.05	0.023 ± 0.000
21h	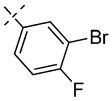	0.84 ± 0.07	0.045± 0.000
21i	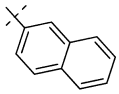	1.3 ± 0.0	0.064 ± 0.010
21j	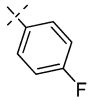	0.071 ± 0.000	0.0034 ± 0.0003
21k	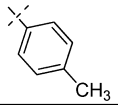	0.33 ± 0.03	0.0090 ± 0.0000

[a]Both IC_{50} values are reported here, as we consider the standard deviation between the replicates to be significant.

antagonists, and to that end, we analyzed the percentages of parent compound remaining at 15, 30, and 60 min after incubation in mouse liver microsomes. We were pleased to learn that **20e** had the lowest rate of intrinsic clearance, which boded well for prospective in vivo studies and was a clear advantage over **1b** and **2**.

The discovery of the potent NPSR antagonist **20e** warranted an in vivo evaluation of its activity. As a preliminary study, we chose to examine the efficacy of this compound in a rat food intake model where the NPSR peptide antagonist [D-Cys-(tBU)^5]NPS was able to reverse the anorectic effect of NPS.[32] While we predicted a reasonable exposure in plasma, we were unsure of the blood–brain barrier penetration of **20e**. Hence, at the outset, we decided to dose **20e** by the intracerebroventricular (ICV) route as well. To that end, Wistar rats were habituated to palatable food consumption and then treated with ICV injections of NPS, which led to a marked reduction in food intake measured at 15, 30, and 60 min. Gratifyingly, a single 10 μg dose of **20e** was able to reverse the suppression of food intake induced by NPS at all three time points (Figure 3).

The success in the food intake in vivo model experiment led to further characterization of **20e**. While ICV administration of the drug was a robust way to check for proof of principle, the evaluation of pharmacokinetics after IP administration of the drug was a more suitable path forward toward more long-term in vivo studies. Table 5 enumerates the exposure levels that were achieved after a 10 mpk dose in mice. In plasma, a C_{max} of 1.5 μM was reached 15 min post dose, and the concentrations steadily declined with a half-life of 8.8 h to about 54 nM at 24 h. More importantly, the drug crossed the blood–brain barrier, and drug levels (52 nM) that were above the in vitro IC_{50} values in all three functional assays were observed even at 24 h. No adverse reactions were observed in this single-dose study. This bodes well for further in vivo characterization of this chemical series in other disease models. While we are aware that the total drug concentration in the brain may not be a good indicator of a pharmacodynamic effect,[33] detailed in vivo studies of **20e** in rat alcohol models showed efficacy with an IP dose of 1.0 mpk.[34]

Compound **20e** was also profiled at 10 μM against 55 targets. We observed >90% inhibition of control in seven targets, which were followed with IC_{50} determination studies (Table 1 in the Supporting Information). We were particularly concerned with the activity in the μ-agonist displacement assay. We decided to compare this activity with those for compounds having potent affinity toward the μ-opioid receptor (Figure 4). Thus, in an in-house assay to monitor the displacement of radiolabeled DAMGO, a peptide with potent affinity for the μ-opioid receptor, we observed that **20e** was more than 200-fold less active than naloxone or morphine. With an IC_{50} of 1 nM in the [^{125}I]NPS displacement assay, it appears that a reasonable therapeutic window exists between the probe's affinities toward NPSR and the μ-opioid receptor.

CONCLUSIONS

The qHTS paradigm at NCGC was used to identify a structurally novel small molecule as an antagonist to the NPS–NPSR neurocircuitry. Further medicinal chemistry revealed the uniqueness of this chemotype toward receptor binding and showed that even slight modifications to the structure resulted in dramatic loss of activity. Simple overlap models with a previously disclosed inhibitor prompted an SAR study that led to the synthesis of the potent analogues **20d** and **20e**. The latter was characterized as a potent antagonist in functional and binding assays. Administration of this compound by the ICV route completely reversed NPS-induced suppression of palatable food intake in rats. In vitro stability studies in mouse liver microsomes showed that this compound has a lower rate of metabolism compared with the most characterized compounds in the literature. This translated to a 10 mpk IP dose in mice, which proved to be safe and maintained high levels of drug in the plasma with slow elimination. This experiment also demonstrated that the drug was able to cross

dx.doi.org/10.1021/jm400904m | J. Med. Chem. XXXX, XXX, XXX–XXX

Table 4. Comparison of Key Potent NPSR Antagonists: The Reported cAMP and Ca^{2+} Assay Activities Are Mean IC_{50} Values from Two Separate Experiments, Each Run in Duplicate; The Reported ERK, [^{125}I]Tyr10-hNPS Displacement, and Microsome Assay Results Are Mean Values from Respective Single Experiments Run in Duplicate

	IC_{50} (nM)				% remaining[a]							
					with NADPH				without NADPH			
#	Ca^{2+}	cAMP	ERK	[^{125}I]Tyr10-hNPS	0	15	30	60	0	15	30	60
1b	5.3	420	14	25	100	29	9	2	98	105	96	101
2	1.2	55	11	6.7	100	0	0	0	96	103	97	94
20e	0.96	45	1.3	3.5	100	72	46	26	94	102	102	102

[a]Percentage of parent compound remaining after incubation in mouse liver microsomes for the indicated times in minutes.

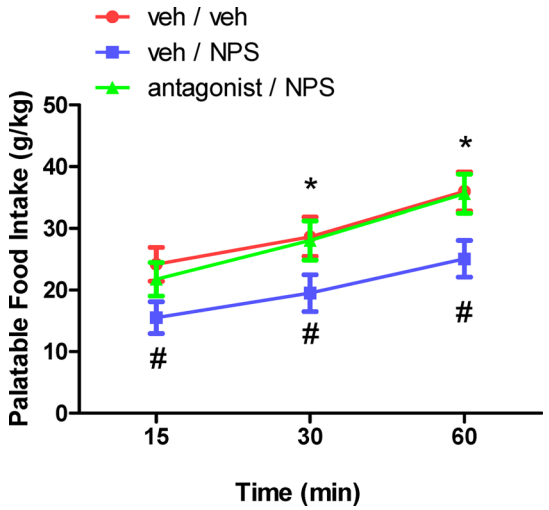

Figure 3. Reversal of NPS-induced suppression of palatable food intake. Three groups of rats (each with $N = 7$) were treated with two successive (10 min apart) 10 μL ICV injections of (a) vehicle (10 μL of 2% DMSO in distilled water) followed by vehicle (veh/veh); (b) vehicle followed by 10 μg of NPS in vehicle (veh/NPS); and (c) 10 μg of **20e** in vehicle followed by 10 μg of NPS in vehicle (antagonist/NPS). Following the second injection, animals were placed back into their cages. Palatable food (17% H_2O, 33% sweetened condensed milk, 51% rat chow) was introduced 20 min thereafter, and intake was measured at the indicated time points. #, $p < 0.5$ veh/NPS group vs veh/veh group; *, $p < 0.05$ antagonist/NPS group vs veh/NPS group.

Table 5. Mouse Pharmacokinetics of 20e[35] (The Concentration at Each Time Point Presented Here Is the Mean Derived from $N = 3$)

	10 mpk IP					
	plasma			brain		
sampling time (h)	mean (ng/mL)[a]	SD (ng/mL)	mean (nM)	mean (ng/g)[a]	SD (ng/g)	mean (nmol/g)
0	BQL	N/A	BQL	BQL	N/A	BQL
0.083	700	306	1503	14	2.41	30
0.25	617	111	1325	24	8.16	52
0.5	536	235	1150	25	3.57	53
1	259	5.03	556	21	5.14	44
2	180	7.64	386	27	6.95	57
4	114	18.3	245	24	3.31	53
8	99	34.6	214	28	8.06	60
12	58	9.66	126	43	17.8	93
24	25	4.33	54	24	2.45	52

PK parameters	plasma	brain
t_{max} (h)	0.083	12
C_{max} (ng/mL)	700	43
$t_{1/2}$ (h)	8.8	N/A
AUC_{last} (h ng/mL)	2240	746
AUC_{inf} (h ng/mL)	2560	N/A
AUC_{brain}/AUC_{plasma} (%)	33	

[a]Mean from $N = 3$

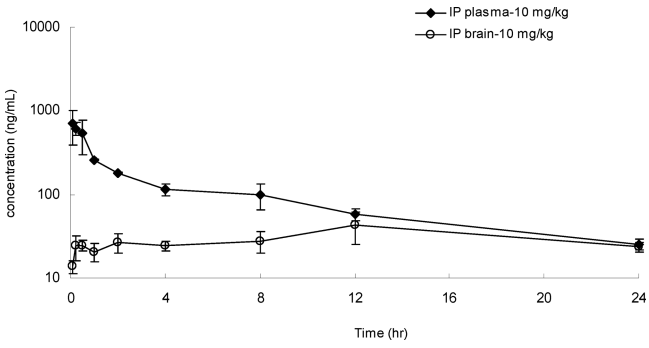

the blood–brain barrier and maintain concentrations higher than the in vitro functional assay IC_{50} for 24 h in the brain. Thus, in spite of its unusual structure, we have described the progression of these phosphorothioyl-containing imidazopyridinium compounds to physiologically relevant antagonists of the NPS/NPSR pathway. Recently, we completed an evaluation of **20e** in animal models of alcoholism, where antagonism of NPSR is predicted to have an effect.[32] The results of these studies showed a suppression of alcohol self-administration in rats with a dose as low as 1 mpk. We also showed that at the same dose, **20e** is able to reduce alcohol-induced ERK phosphorylation in the central amygdala of these rats.

EXPERIMENTAL SECTION

cAMP Assay. A Chinese hamster ovary cell line stably expressing the NPSR was generated in the Heilig lab. The cells were maintained in F12 medium containing 10% FBS, 100 units/mL penicillin, 100 μg/mL streptomycin, and 200 μg/mL geneticin at 37 °C, 5% CO_2. Suspended CHO-NPSR cells were seeded into 1536-well tissue-culture-treated white plates at a density of 1800 cells/well in 4 μL of medium without geneticin and incubated at 37 °C, 5% CO_2 overnight. After 1 μL of stimulation buffer (1× PBS, 0.1% BSA, 0.05% Tween-20, 500 μM Ro 20-1724, EC80 of NPS) was added to each well, cells were incubated at 37 °C, 5% CO_2 for 30 min. D2-conjugated cAMP (1.25 μL) and cryptate-conjugated anti-cAMP antibody (1 μf) were then added. D2-conjugated cAMP and cryptate-conjugated anti-cAMP antibody were both prepared in cell lysis buffer according to the manufacturer's instructions. After 30 min, the plates were then read with a Viewlux plate reader (PerkinElmer) using the TRF detection mode optimized for HTRF. This assay was done routinely as compounds were generated. The reported data are mean IC_{50} values with SDs from two independent experiments, each run in duplicate.

ERK Assay. CHO-NPSR cells were cultured using F12K medium (ATCC) supplemented with 10% FBS and 250 μg/mL hygromycin b

dx.doi.org/10.1021/jm400904m | J. Med. Chem. XXXX, XXX, XXX–XXX

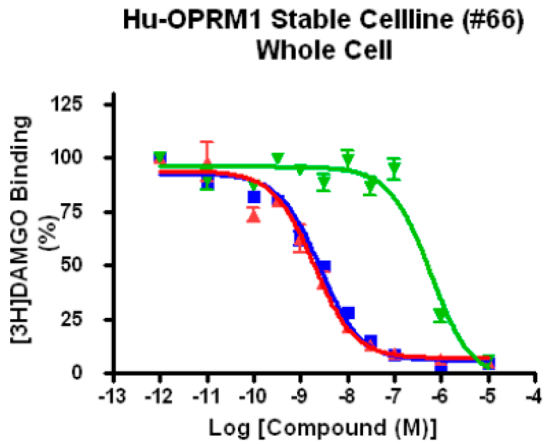

Figure 4. μ-Opioid receptor affinity of **20e** compared with those of naloxone and morphine in the human recombinant μ-opioid receptor OPRM1 stable cell line: (blue curve) morphine, IC_{50} = 2.5 ± 0.05 nM; (red curve) naloxone, IC_{50} = 1.87 ± 0.07 nM; (green curve) **20e**, IC_{50} = 580 ± 0.11 nM.

(Life Technologies) selection antibiotic. Cells were harvested in Opti-MEM (ATCC) supplemented with 1% FBS and plated in Greiner 96-well white tissue-culture-treated clear-bottom plates at a seeding density of 25 000 cells/well and grown overnight at 37 °C, 5% CO_2. The medium in the wells was replaced with 100 μL of Opti-MEM only, and the cells were incubated at 37 °C, 5% CO_2 for an additional 4 h. A 1 μL aliquot of compound (at the appropriate dilution in DMSO) was added to each well and incubated for 10 min. A 100 μL aliquot of 1 nM NPS final concentration (EC80) was added to every well prepared in Opti-MEM supplemented with 0.2% BSA and 0.005% Tween-20 (Sigma). After incubation for 20 min, all of the medium was removed, and the plate was placed on ice for 5 min. The Cellul'erk kit (Cisbio) instructions were then followed. Briefly, 50 μL of 1× lysis solution was added per well and incubated at room temperature with gentle rocking for 15 min. Lysed cells (16 μL) were transferred to Greiner white medium binding half-well plates. A 1× solution of deuterium-conjugated anti-ERK1/2 antibody (2 μL per well) was added and incubated for 2 h at room temperature in the dark. A 1× solution of europium cryptate-conjugated anti−ERK1/2 antibody (2 μL per well) was added and incubated overnight at ambient temperature in the dark. The plate was read using HTRF settings on an EnVision reader (PerkinElmer). The reported ERK assay activities are mean IC_{50} values with SDs from one experiment run in duplicate.

Calcium Assay. The CHO-NPSR cell line used in the cAMP assay was also used in this calcium mobilization assay. The suspended cells were plated at 3 μL/well with 2000 cells in black tissue-culture-treated clear-bottom 1536-well plates. After overnight incubation at 37 °C, 5% CO_2, 3 μL of the calcium dye (no-wash High Performance PBX Calcium Assay Kit, BD Biosciences) was loaded into each well, and the plates were incubated at 37 °C, 5% CO_2 for 1 h followed by incubation for 10 min with 23 nL of compound prepared in DMSO solution. The assay plates were then placed onto the FDSS-7000 kinetic fluorescence plate reader for measurement of the changes in intracellular free calcium. The basal fluorescence signal was recorded for 6 s at 1 Hz followed by the addition of 1 μL of NPS stimulation buffer (1× PBS, 0.1% BSA, 0.05% Tween-20, 500 μM Ro 20-1724, EC80 of NPS) and continuous recording at 1 Hz for 4 min. This assay was done routinely as compounds were generated. The reported data are mean IC_{50} values with SDs from two independent experiments, each run in duplicate.

[^{125}I]Tyr10-hNPS Binding Assay. The assay was carried out as described earlier with minor modification.[3] Y10-NPS labeled with ^{125}I was bought from NEN PerkinElmer (Boston, MA). CHO cells stably expressing human NPSR were seeded into 24-well plates and cultured until they reached 90−95% confluency. The cells were washed once with 1 mL of PBS and then incubated with radioligand with or without compounds or in DMEM containing 0.1% BSA at 20 °C for 1.5 h. Increasing concentrations of compounds or unlabeled human NPS were used to compete with 0.15 nM [^{125}I]Y10-NPS. Nonspecific binding was determined in the presence of 1 μM unlabeled human NPS. Cells were washed twice with cold PBS and lysed with 1 N NaOH. Bound radioactivity was counted in a liquid scintillation counter. The reported activities are mean IC_{50} values with SDs from one experiment run in duplicate.

General Methods. Unless otherwise stated, reactions were carried out under an atmosphere of dry argon or nitrogen in dried glassware. The indicated reaction temperatures refer to the reaction bath, while room temperature (rt) is noted as ~25 °C. All anhydrous solvents, commercially available starting materials, and reagents were purchased from Aldrich Chemical Co. and used as received. Analytical thin-layer chromatography (TLC) was performed with Sigma-Aldrich TLC plates (5 cm × 20 cm, 60 Å, 250 μm). Visualization was accomplished by irradiation under a 254 nm UV lamp. Chromatography on silica gel was performed using forced flow (liquid) of the indicated solvent system on Biotage KP-Sil prepacked cartridges and a Biotage SP-1 automated chromatography system. Reversed-phase preparative purification was performed on a Waters semipreparative HPLC instrument. The column used was a Phenomenex Luna C18 (5 μm, 30 mm × 75 mm) at a flow rate of 45 mL/min. The mobile phase consisted of acetonitrile and water (each containing 0.1% trifluoroacetic acid). A gradient of 10% to 50% acetonitrile over 8 min was used during the purification. Fraction collection was triggered by UV detection (220 nM). ^{1}H spectra were recorded on a Varian Inova 400 MHz spectrometer. Chemical shifts are reported in parts per million with the solvent resonance as the internal standard ($CDCl_3$ 7.27 ppm and DMSO-d_6 2.50 ppm for ^{1}H). Data are reported as follows: chemical shift, multiplicity (s = singlet, d = doublet, t = triplet, q = quartet, br s = broad singlet, m = multiplet), coupling constant(s), number of protons.

The reported analytical purity analyses and retention times were obtained by the following two methods on an Agilent LC/MS (Agilent Technologies, Santa Clara, CA): Method 1: A 7 min gradient of 4% to 100% acetonitrile (containing 0.025% trifluoroacetic acid) in water (containing 0.05% trifluoroacetic acid) was used with an 8 min run time at a flow rate of 1 mL/min. A Phenomenex Luna C18 column (3 μm, 3 mm × 75 mm) was used at a temperature of 50 °C. Method 2: A 3 min gradient of 4% to 100% acetonitrile (containing 0.025% trifluoroacetic acid) in water (containing 0.05% trifluoroacetic acid) was used with a 4.5 min run time at a flow rate of 1 mL/min. A Phenomenex Luna C18 column (3 μm, 3 mm × 100 mm) was used at a temperature of 50 °C. Unless otherwise stated, analogues were determined to have >95% purity using the above methods.

Mass determinations were performed using an Agilent 6130 mass spectrometer with electrospray ionization in the positive mode. Molecular weights were confirmed using an Agilent time-of-flight (TOF) mass spectrometer. A 3 min gradient from 4% to 100% acetonitrile (0.1% formic acid) in water (0.1% formic acid) was used with a 4 min run time at a flow rate of 1 mL/min. A Zorbax SB-C18 column (3.5 μm, 2.1 mm × 30 mm) was used at a temperature of 50 °C. Molecular formulas were confirmed using electrospray ionization in the positive mode with the Agilent Masshunter software (version B.02).

2-Amino-1-(prop-2-yn-1-yl)pyridin-1-ium Bromide (9). Pyridin-2-amine (9.5 g, 0.10 mol) and 3-bromoprop-1-yne (10 mL, 0.10 mol) were added to ethanol (50 mL) and refluxed for 2 h. The reaction was left to cool overnight. A light-yellow solid precipitated out of the reaction mixture. This was filtered via a Buchner funnel, washed with cold ethanol, and air-dried to obtain 2-amino-1-(prop-2-ynyl)pyridinium bromide (10 g, 47 mmol, 47% yield). ^{1}H NMR (400 MHz, DMSO-d_6): δ 3.82 (t, J = 2.5 Hz, 1H), 5.08 (d, J = 2.5 Hz, 2H), 6.95 (td, J = 6.9, 1.4 Hz, 1H), 7.11 (m, 1H), 7.91 (ddd, J = 8.9, 7.1, 1.7 Hz, 1H), 8.17 (m, 1H), 8.63 (br s, 2H).

2-Methylimidazo[1,2-*a*]pyridine (10b). 2-Amino-1-(prop-2-yn-1-yl)pyridinium bromide **9** (6.0 g, 28 mmol) was mixed with copper(I) iodide (0.537 g, 2.82 mmol) and $PdCl_2(PPh_3)_2$ (0.495 g, 0.705 mmol) in DMF (50 mL). The mixture was treated with

dx.doi.org/10.1021/jm400904m | J. Med. Chem. XXXX, XXX, XXX−XXX

triethylamine (12 mL, 87 mmol) and stirred overnight, during which the light-orange solution turned brown. The reaction mixture was concentrated, adsorbed onto silica gel, and then purified by flash silica gel chromatography (0 to 100% DCM/EtOAc) to provide 2-methylimidazo[1,2-*a*]pyridine (2.69 g, 20.4 mmol, 70.5% yield). ^{1}H NMR (400 MHz, $CDCl_3$): δ 2.46 (s, 3H), 6.72 (m, 1H), 7.11 (ddd, J = 9.0, 6.8, 1.4 Hz, 1H), 7.33 (s, 1H), 7.54 (m, 1H), 8.03 (dt, J = 6.8, 1.2 Hz, 1H).

3-(Diphenylphosphino)imidazo[1,2-*a*]pyridine (11a). Chlorodiphenylphosphine (1.40 g, 6.35 mmol) and iodotrimethylsilane (1.27 g, 6.35 mmol) were mixed in toluene (4 mL) and stirred for about 2 h. This mixture was transferred to a premixed solution of imidazo[1,2-*a*]pyridine (500 mg, 4.23 mmol) and triethylamine (2.35 mL, 16.9 mmol) in pyridine (10 mL). The reaction mixture was allowed to stir overnight, concentrated in vacuo, and concentrated with toluene (×2) to remove pyridine. The crude mixture was dissolved in DCM and purified by silica gel chromatography (0 to 100% EtOAc/DCM) to provide 3-(diphenylphosphino)imidazo [1,2-*a*]pyridine (550 mg, 1.82 mmol, 43.0% yield). ^{1}H NMR (400 MHz, DMSO-d_6): δ 6.94 (td, J = 6.8, 1.4 Hz, 1H), 7.36 (m, 12H), 7.71 (m, 1H), 8.16 (m, J = 6.8, 2.1, 1.1, 1.1 Hz, 1H). LC/MS: method 1, retention time 4.500 min. HRMS (m/z): calcd for $C_{19}H_{16}N_2P^+$ $(M + H)^+$ 303.1046, found 303.1049.

3-(Diphenylphosphoryl)imidazo[1,2-*a*]pyridine HCl (12a). 3-(Diphenylphosphino)imidazo[1,2-*a*]pyridine **11a** (125 mg, 0.413 mmol) was dissolved in THF and treated with excess 30% hydrogen peroxide (300 mg, 2.65 mmol). The mixture was stirred for 16 h and then diluted with EtOAc and washed with water. The organic layer was dried ($MgSO_4$), filtered, concentrated, and purified by reversed-phase HPLC. The TFA salt obtained was dissolved in CH_2Cl_2, treated with excess HCl (4 M in Et_2O), and then concentrated in vacuo (twice) to obtain the HCl salt of 3-(diphenylphosphoryl)imidazo[1,2-*a*]pyridine (45 mg, 0.13 mmol, 31% yield). ^{1}H NMR (400 MHz, DMSO-d_6): δ 7.39 (m, 1H), 7.63 (m, 4H), 7.75 (m, 6H), 7.87 (m, 1H), 7.94 (s, 1H), 8.00 (m, 1H), 8.78 (d, J = 6.8 Hz, 1H). LC/MS: method 1, retention time 3.693 min. HRMS (m/z): calcd for $C_{19}H_{16}N_2OP$ $(M + H)^+$ 319.0995, found 319.0995.

3-(Diphenylphosphorothioyl)imidazo[1,2-*a*]pyridine HCl (12b). 3-(Diphenylphosphino)imidazo [1,2-*a*]pyridine **11a** (125 mg, 0.413 mmol) was dissolved in THF and treated with excess sulfur (50 mg, 1.6 mmol). The mixture was stirred for 16 h and then diluted with EtOAc and washed with water. The organic layer was dried ($MgSO_4$), filtered, concentrated, and purified by reversed-phase HPLC. The TFA salt obtained was dissolved in CH_2Cl_2, treated with excess HCl (4 M in Et_2O), and then concentrated in vacuo (twice) to obtain the HCl salt of 3-(diphenylphosphorothioyl)imidazo[1,2-*a*]pyridine (50 mg, 0.135 mmol, 33% yield). ^{1}H NMR (400 MHz, DMSO-d_6): δ 7.19 (t, J = 6.8 Hz, 1H), 7.38 (br s, 1H), 7.66 (m, 7H), 7.80 (m, 4H), 7.89 (d, J = 9.2 Hz, 1H), 8.52 (d, J = 6.7 Hz, 1H). LC/MS: method 1, retention time 4.845 min. HRMS (m/z): calcd for $C_{19}H_{16}N_2PS$ $(M + H)^+$ 335.0766, found 335.0771.

3-(Diphenylphosphoryl)-2-methylimidazo[1,2-*a*]pyridine HCl (12c). Compound **12c** could be prepared from 2-methylimidazo-[1,2-*a*]pyridine **10b** using the procedure to make **12a** or by the following procedure: 3-Bromo-2-methylimidazo[1,2-*a*]pyridine (290 mg, 1.37 mmol, not completely pure) was dissolved in THF (5 mL), and the solution was cooled to −15 °C under nitrogen. Isopropylmagnesium chloride·lithium chloride (2 mL, 2 mmol) was added, and the mixture was allowed to warm to 10 °C, at which point it was determined by TLC (1:1 DCM/EtOAc) that the halogen−metal exchange was complete. A solution of chlorodiphenylphosphine (300 mg, 1.36 mmol) in THF (1 mL) was added via syringe, and the reaction mixture was allowed to gradually warm to rt. The reaction was quenched by addition of sat aq. NH_4Cl, and the mixture was extracted with EtOAc. The organic layer was separated and purified by silica gel chromatography (0 to 100% EtOAc/DCM). The product, which was not completely pure as judged by ^{1}H NMR analysis, was added to THF,treated with excess 30% hydrogen peroxide, and stirred overnight. Water was added, and the mixture was extracted with EtOAc and concentrated, after which the residue was purified by reversed-phase HPLC. The fractions were treated with sat. aq. $NaHCO_3$, extracted with EtOAc, dried ($MgSO_4$), filtered, concentrated, redissolved in DCM, and converted to the purported HCl salt by treatment with excess 1 M HCl in Et_2O followed by concentration. The residue was redissolved in DCM and treated with Et_2O to cause precipitation. The solid obtained was filtered and washed with Et_2O to obtain 3-(diphenylphosphoryl)-2-methylimidazo[1,2-*a*]pyridine HCl (30 mg, 0.08 mmol, 5.9% yield). ^{1}H NMR (400 MHz, DMSO-d_6): δ 1.82 (d, J = 1.2 Hz, 3H), 7.24 (m, 1H), 7.68 (m, 11H), 7.85 (d, J = 8.6 Hz, 1H), 8.84 (d, J = 6.7 Hz, 1H). LC/MS: method 1, retention time 3.734 min. HRMS (m/z): calcd for $C_{20}H_{18}N_2OP^+$ $(M + H)^+$ 333.1151, found 333.1157.

3-(Diphenylphosphorothioyl)-2-methylimidazo[1,2-*a*]-pyridine (12d) (General Procedure A). Chlorodiphenylphosphine (3.89 mL, 26.4 mmol) and iodotrimethylsilane (5.29 g, 26.4 mmol) were stirred in toluene (10 mL) for 2 h. This mixture was added to a premixed solution of 2-methylimidazo[1,2-*a*]pyridine **10b** (2.33 g, 17.6 mmol) and triethylamine (9.78 mL, 70.5 mmol) in pyridine (10.0 mL), and the resulting mixture was stirred for 12 h. Sulfur (0.565 g, 17.6 mmol) was added, and the mixture was stirred for another 6 h, concentrated, concentrated again with toluene (to remove pyridine), and diluted with benzene. The solids (presumed to be Et_3N and pyridine salts) were filtered, and the filtrate was adsorbed over silica and subjected to purification by flash silica gel chromatography (0 to 75% EtOAc in DCM) to provide 3-(diphenylphosphorothioyl)-2-methylimidazo[1,2-*a*]pyridine (3.02 g, 8.67 mmol, 49.2% yield). ^{1}H NMR (400 MHz, DMSO-d_6): δ 1.57 (m, 3H), 6.96 (m, J = 6.7, 6.7, 1.0, 0.7 Hz, 1H), 7.44 (m, 1H), 7.60 (m, 4H), 7.68 (m, 3H), 7.78 (m, 4H), 8.35 (dt, J = 6.8, 1.2 Hz, 1H).

3-(Diphenylphosphorothioyl)-1,2-dimethyl-1*H*-imidazo[1,2-*a*]pyridin-1-ium Methyl Sulfate (13b) (General Procedure B). 3-(Diphenylphosphorothioyl)-2-methylimidazo[1,2-*a*]pyridine **12d** (90 mg, 0.26 mmol) and dimethyl sulfate (0.05 mL, 0.52 mmol) were added to dioxane (2 mL). The mixture was heated in a sealed tube at 100 °C for 16 h and then cooled. The solid obtained was filtered, washed with diethyl ether, and air-dried to obtain 3-(diphenylphosphorothioyl)-1,2-dimethyl-1*H*-imidazo[1,2-*a*]pyridin-1-ium methyl sulfate (50 mg, 0.11 mmol, 41% yield). ^{1}H NMR (400 MHz, DMSO-d_6): δ 1.67 (m, 3H), 3.91 (s, 3H), 7.54 (t, J = 7.0 Hz, 1H), 7.68 (td, J = 7.6, 3.5 Hz, 4H), 7.77 (m, 2H), 7.87 (m, 4H), 8.15 (t, J = 8.3 Hz, 1H), 8.39 (m, 1H), 8.66 (d, J = 6.8 Hz, 1H). LC/MS: method 1, retention time 4.545 min. HRMS (m/z): calcd for $C_{21}H_{20}N_2PS^+$ $(M)^+$ 363.1079, found 363.1080.

3-(Diphenylphosphorothioyl)-1-methyl-1*H*-imidazo[1,2-*a*]-pyridin-1-ium Methyl Sulfate (13a). 3-(Diphenylphosphorothioyl)imidazo[1,2-*a*]pyridine **12b** (150 mg, 0.449 mmol) was reacted with dimethyl sulfate (0.086 mL, 0.897 mmol) according to general procedure B to obtain 3-(diphenylphosphorothioyl)-1-methyl-1*H*-imidazo[1,2-*a*]pyridin-1-ium methyl sulfate (70 mg, 0.15 mmol, 34% yield). ^{1}H NMR (400 MHz, DMSO-d_6): δ 4.02 (s, 3H), 7.65 (m, 5H), 7.77 (m, 2H), 7.86 (m, 4H), 8.08 (dd, J = 2.0, 0.4 Hz, 1H), 8.21 (m, 1H), 8.3 (m, 1H), 8.72 (m, 1H). LC/MS: method 1, retention time 4.468 min. HRMS (m/z): calcd for $C_{20}H_{18}N_2PS^+$ $(M)^+$ 349.0923, found 349.0925.

Imidazo[1,2-*a*]pyridin-3-yldiphenylmethanol (18a). 3-Bromoimidazo[1,2-*a*]pyridine (172 mg, 0.873 mmol) **17a** was dissolved in THF (5 mL), and the solution was cooled to −15 °C under nitrogen. Isopropylmagnesium chloride·lithium chloride (1.5 mL, 1.5 mmol) was added, and the mixture was gradually warmed to 10 °C. A solution of benzophenone (175 mg, 0.960 mmol) in THF (1 mL) was added via syringe, and the solution was warmed to rt. The reaction was quenched by addition of sat aq. NH_4Cl, and the resulting solution was extracted with EtOAc. The organic layer was separated, concentrated, and purified by reversed-phase HPLC, which provided the TFA salt. This was converted to its free base by dissolution in EtOAc followed by treatment with sat aq. $NaHCO_3$. The organic phase was dried ($MgSO_4$), filtered, and concentrated. The oily residue was dissolved in minimal CH_2Cl_2, treated with Et_2O, and sonicated to cause precipitation of a solid, which was filtered and air-dried to provide imidazo[1,2-*a*]pyridin-3-yldiphenylmethanol (80 mg, 0.27

dx.doi.org/10.1021/jm400904m | *J. Med. Chem.* XXXX, XXX, XXX−XXX

mmol, 18% yield). ^{1}H NMR (400 MHz, $CDCl_3$): δ 3.05 (s, 1H), 6.63 (m, 1H), 7.01 (s, 1H), 7.18 (m, 1H), 7.35 (m, 8H), 7.61 (m, 1H), 8.06 (m, 1H). LC/MS: method 1, retention time 4.143 min. HRMS (m/z): calcd for $C_{20}H_{17}N_2O^+$ $(M + H)^+$ 301.1335, found 301.1337.

(2-Methylimidazo[1,2-*a*]pyridin-3-yl)diphenylmethanol (18b). 3-Bromo-2-methylimidazo[1,2-*a*]pyridine (220 mg, 1.04 mmol, not completely pure) was dissolved in THF (5 mL), and the solution was cooled to −15 °C under nitrogen. Isopropylmagnesium chloride·lithium chloride (2.7 mL, 2.70 mmol) was added, and the mixture was allowed to warm to 10 °C. A solution of benzophenone (208 mg, 1.141 mmol) in THF (1 mL) was added via syringe, and the solution warmed to rt. The reaction was quenched by addition of sat. aq. NH_4Cl, and the resulting solution was extracted with EtOAc. The organic layer was separated and then purified by silica gel chromatography (0 to 100% EtOAc in DCM) to provide (2-methylimidazo[1,2-*a*]pyridin-3-yl)diphenylmethanol (100 mg, 0.318 mmol, 30.5% yield). ^{1}H NMR (400 MHz, DMSO-d_6): δ 1.38 (s, 3H), 6.65 (m, 1H), 6.93 (s, 1H), 7.14 (ddd, J = 9.0, 6.7, 1.4 Hz, 1H), 7.23 (m, 4H), 7.33 (m, 6H), 7.43 (dt, J = 9.0, 1.2 Hz, 1H), 8.11 (dt, J = 7.0, 1.3 Hz, 1H). LC/MS: method 1, retention time 4.290 min. HRMS (m/z): calcd for $C_{21}H_{19}N_2O^+$ $(M + H)^+$ 315.1492, found 315.1495.

3-(Hydroxydiphenylmethyl)-1,2-dimethylimidazo[1,2-*a*]pyridin-1-ium Trifluoroacetate (19b) (General Procedure C). A solution of (2-Methylimidazo[1,2-*a*]pyridin-3-yl)diphenylmethanol (32 mg, 0.102 mmol) and dimethyl sulfate (15 μL, 0.157 mmol) in dioxane (3.0 mL) was heated in a sealed tube overnight. An oily residue suspended in dioxane was observed. The mixture was concentrated, purified with reversed-phase HPLC (25 to 70% MeCN in water, 0.1% TFA) to provide 3-(hydroxydiphenylmethyl)-1,2-dimethylimidazo[1,2-*a*]pyridin-1-ium trifluoroacetate (25 mg, 0.057 mmol, 56% yield) . The methyl sulfate counteranion was assumed to be exchanged for trifluoroacetate. ^{1}H NMR (400 MHz, DMSO-d_6): δ 1.49 (s, 3H), 3.88 (s, 3H), 7.37 (m, 11H), 7.60 (m, 1H), 7.99 (m, 1H), 8.25 (d, J = 9.2 Hz, 1H), 8.58 (d, J = 7.0 Hz, 1H). LC/MS: method 1, retention time 4.321 min. HRMS (m/z): calcd for $C_{22}H_{21}N_2O^+$ $(M)^+$ 329.1648, found 329.1656.

3-(Hydroxydiphenylmethyl)-1-methylimidazo[1,2-*a*]pyridin-1-ium Trifluoroacetate (19a). Imidazo[1,2-*a*]pyridin-3-yldiphenylmethanol **18a** (48 mg, 0.16 mmol) and dimethyl sulfate (25 μL, 0.26 mmol) were reacted according to general procedure C to obtain 3-(hydroxydiphenylmethyl)-1-methylimidazo[1,2-*a*]pyridin-1-ium trifluoroacetate (35 mg, 0.082 mmol, 51% yield). ^{1}H NMR (400 MHz, DMSO-d_6): δ 7.41 (m, 11H), 7.56 (s, 1H), 8.05 (ddd, J = 9.1, 7.1, 1.2 Hz, 1H), 8.24 (dt, J = 9.2, 1.1 Hz, 1H), 8.39 (m, 1H). LC/MS: method 1, retention time 4.074 min. HRMS (m/z): calcd for $C_{21}H_{19}N_2O^+$ $(M)^+$ 315.1492, found 315.1497.

3-(Diphenylphosphorothioyl)-1,2-dimethyl-1*H*-indole (15b). Chlorodiphenylphosphine, iodotrimethylsilane, commercially available 1,2-dimethyl-1*H*-indole, and triethylamine were reacted according to general procedure A to obtain 3-(diphenylphosphorothioyl)-1,2-dimethyl-1*H*-indole in 40% yield. ^{1}H NMR (400 MHz, DMSO-d_6): δ 2.17 (d, J = 1.4 Hz, 3H), 3.72 (s, 3H), 6.36 (dt, J = 8.0, 1.0 Hz, 1H), 6.78 (ddd, J = 8.2, 7.1, 1.2 Hz, 1H), 7.10 (ddd, J = 8.2, 7.0, 1.2 Hz, 1H), 7.53 (m, 5H), 7.59 (m, 2H), 7.82 (m, 4H). LC/MS: method 1, retention time 6.915 min. HRMS (m/z): calcd for $C_{22}H_{21}NPS^+$ $(M + H)^+$ 362.1127, found 362.1134.

3-(Diphenylphosphorothioyl)-1-methyl-1*H*-indole (15a). Chlorodiphenylphosphine, iodotrimethylsilane, 1-methyl-1*H*-indole, triethylamine, and sulfur were reacted according to general procedure A to produce 3-(diphenylphosphorothioyl)-1-methyl-1*H*-indole in 39% yield. ^{1}H NMR (400 MHz, DMSO-d_6): δ 3.85 (s, 3H), 7.05 (ddd, J = 8.1, 7.0, 1.1 Hz, 1H), 7.25 (ddd, J = 8.3, 7.1, 1.3 Hz, 1H), 7.30 (dt, J = 8.0, 1.0 Hz, 1H), 7.44 (d, J = 4.5 Hz, 1H), 7.56 (m, 7H), 7.74 (m, 4H). LC/MS: method 1, retention time 6.793 min. HRMS (m/z): calcd for $C_{21}H_{19}NPS^+$ $(M + H)^+$ 348.0970, found 348.0974.

Compounds 20a–g and 21a–k. These compounds were prepared by general procedure B or C.

*1-Benzyl-3-(diphenylphosphorothioyl)-2-methylimidazo[1,2-a]pyridin-1-ium Trifluoroacetate (**20a**).* ^{1}H NMR (400 MHz, DMSO-d_6): δ 1.64 (m, 3H), 5.76 (m, 2H), 7.30 (m, 2H), 7.39 (m, 3H), 7.60 (m, 1H), 7.68 (m, 4H), 7.77 (m, 2H), 7.91 (m, 4H), 8.19 (m, 1H), 8.44 (m, 1H), 8.70 (d, J = 6.8 Hz, 1H). LC/MS: method 1, retention time 5.160 min. HRMS (m/z): calcd for $C_{27}H_{24}N_2PS^+$ $(M)^+$ 439.1392, found 439.1398.

*3-(Diphenylphosphorothioyl)-2-methyl-1-phenethylimidazo[1,2-a]pyridin-1-ium Bromide (**20b**).* ^{1}H NMR (400 MHz, DMSO-d_6): δ 1.41 (d, J = 1.4 Hz, 3H), 3.07 (t, J = 6.6 Hz, 2H), 4.66 (t, J = 6.8 Hz, 2H), 7.11 (m, 2H), 7.23 (m, 3H), 7.49 (td, J = 7.1, 1.3 Hz, 1H), 7.66 (m, 4H), 7.78 (m, 6H), 8.04 (m, 1H), 8.22 (m, 1H), 8.65 (m, 1H). LC/MS: method 1, retention time 5.180 min. HRMS (m/z): calcd for $C_{28}H_{26}N_2PS^+$ $(M)^+$ 453.1549, found 453.1555.

*3-(Diphenylphosphorothioyl)-2-methyl-1-(1-oxo-2-phenylethyl)-imidazo[1,2-a]pyridin-1-ium Bromide (**20c**).* ^{1}H NMR (400 MHz, DMSO-d_6): δ 1.62 (s, 3H), 6.37 (s, 2H), 7.66 (m, 7H), 7.79 (m, 3H), 7.91 (m, 4H), 8.11 (dd, J = 8.4, 1.4 Hz, 2H), 8.18 (m, 1H), 8.44 (m, 1H), 8.76 (d, J = 6.8 Hz, 1H). LC/MS: method 1, retention time 5.391 min. HRMS (m/z): calcd for $C_{28}H_{24}N_2OPS^+$ $(M)^+$ 467.1341, found 467.1346.

*3-(Diphenylphosphorothioyl)-2-methyl-1-(3-phenylpropyl)-imidazo[1,2-a]pyridin-1-ium Trifluoroacetate (**20d**).* ^{1}H NMR (400 MHz, DMSO-d_6): δ 1.65 (m, 3H), 2.05 (qd, J = 8.0, 7.7 Hz, 2H), 2.71 (m, 2H), 4.42 (t, J = 7.7 Hz, 2H), 7.17 (m, 5H), 7.52 (tt, J = 7.0, 0.6 Hz, 1H), 7.64 (m, 4H), 7.74 (m, 2H), 7.83 (m, 4H), 8.13 (m, 1H), 8.41 (m, 1H), 8.62 (d, J = 7.0 Hz, 1H). LC/MS: method 1, retention time 5.407 min. HRMS (m/z): calcd for $C_{29}H_{28}N_2PS^+$ $(M)^+$ 467.1705, found 467.1709.

*1-Cinnamyl-3-(diphenylphosphorothioyl)-2-methylimidazo[1,2-a]pyridin-1-ium Bromide (**20e**).* ^{1}H NMR (400 MHz, DMSO-d_6): δ 1.75 (d, J = 1.4 Hz, 3H), 5.28 (m, 2H), 6.43 (m, 1H), 6.86 (d, J = 16.0 Hz, 1H), 7.32 (m, 3H), 7.44 (m, 2H), 7.59 (td, J = 7.1, 1.3 Hz, 1H), 7.68 (m, 4H), 7.78 (m, 2H), 7.91 (m, 4H), 8.20 (ddd, J = 9.2, 7.2, 1.2 Hz, 1H), 8.48 (m, 1H), 8.70 (m, 1H). LC/MS: method 1, retention time 5.744 min. HRMS (m/z): calcd for $C_{29}H_{26}N_2PS^+$ $(M)^+$ 465.1549, found 465.1553.

*3-(Diphenylphosphorothioyl)-2-methyl-1-(4-phenylbutyl)-imidazo[1,2-a]pyridin-1-ium Bromide (**20f**).* ^{1}H NMR (400 MHz, DMSO-d_6): δ 1.73 (m, 7H), 2.62 (m, 2H), 4.43 (m, 2H), 7.18 (m, 3H), 7.28 (m, 2H), 7.55 (td, J = 7.0, 1.4 Hz, 1H), 7.68 (m, 4H), 7.78 (m, 2H), 7.89 (m, 4H), 8.15 (ddd, J = 9.1, 7.1, 1.2 Hz, 1H), 8.42 (dd, J = 9.1, 1.1 Hz, 1H), 8.64 (m, 1H). LC/MS: method 1, retention time 5.638 min. HRMS (m/z): calcd for $C_{30}H_{30}N_2PS^+$ $(M)^+$ 481.1868, found 481.1871.

*3-(Diphenylphosphorothioyl)-2-methyl-1-(5-phenylpentyl)-imidazo[1,2-a]pyridin-1-ium Trifluoroacetate (**20g**).* ^{1}H NMR (400 MHz, DMSO-d_6): δ 1.39 (m, 2H), 1.61 (m, 2H), 1.70 (s, 3H), 1.76 (m, 2H), 2.57 (t, J = 7.4 Hz, 2H), 4.39 (t, J = 7.7 Hz, 2H), 7.16 (m, 3H), 7.26 (m, 2H), 7.55 (m, 1H), 7.68 (td, J = 7.6, 3.5 Hz, 4H), 7.78 (m, 2H), 7.89 (ddd, J = 14.7, 8.3, 1.3 Hz, 4H), 8.15 (m, 1H), 8.43 (m, 1H), 8.65 (d, J = 7.0 Hz, 1H). LC/MS: method 1, retention time 5.738 min. HRMS (m/z): calcd for $C_{31}H_{32}N_2PS^+$ $(M)^+$ 495.2030, found 495.2033.

*(E)-3-(Diphenylphosphorothioyl)-1-(3-(3-methoxyphenyl)allyl)-2-methylimidazo[1,2-a]pyridin-1-ium Trifluoroacetate (**21a**).* ^{1}H NMR (400 MHz, DMSO-d_6): δ 1.75 (d, J = 1.4 Hz, 3H), 3.75 (s, 3H), 5.27 (m, 2H), 5.75 (s, 1H), 6.86 (m, 2H), 7.01 (m, 2H), 7.26 (m, 1H), 7.59 (m, 1H), 7.69 (m, 4H), 7.78 (td, J = 7.6, 1.6 Hz, 2H), 7.91 (ddd, J = 14.7, 8.4, 1.4 Hz, 4H), 8.20 (m, 1H), 8.48 (d, J = 9.2 Hz, 1H), 8.70 (m, 1H). LC/MS: method 1, retention time 5.305 min. HRMS (m/z): calcd for $C_{30}H_{28}N_2OPS^+$ $(M)^+$ 495.1661, found 495.1661.

*(E)-1-(3-(2-Chlorophenyl)allyl)-3-(diphenylphosphorothioyl)-2-methylimidazo[1,2-a]pyridin-1-ium Trifluoroacetate (**21b**).* ^{1}H NMR (400 MHz, DMSO-d_6): δ 1.76 (d, J = 1.4 Hz, 3H), 5.39 (m, 2H), 6.46 (dt, J = 15.8, 6.2 Hz, 1H), 7.10 (d, J = 16.0 Hz, 1H), 7.33 (m, 2H), 7.46 (m, 1H), 7.65 (m, 6H), 7.78 (m, 2H), 7.91 (m, 4H), 8.21 (ddd, J = 8.9, 7.3, 1.2 Hz, 1H), 8.50 (dd, J = 9.2, 1.2 Hz, 1H), 8.70 (m, 1H). LC/MS: method 1, retention time 5.440 min. HRMS (m/z): calcd for $C_{29}H_{25}ClN_2PS^+$ $(M)^+$ 499.1168, found 499.1170.

*(E)-1-(3-(3-Chlorophenyl)allyl)-3-(diphenylphosphorothioyl)-2-methylimidazo[1,2-a]pyridin-1-ium Trifluoroacetate (**21c**).* ^{1}H NMR (400 MHz, DMSO-d_6): δ 1.75 (m, 3H), 5.29 (m, 2H), 6.53

dx.doi.org/10.1021/jm400904m | J. Med. Chem. XXXX, XXX, XXX−XXX

(dt, J = 15.9, 6.1 Hz, 1H), 6.82 (d, J = 15.8 Hz, 1H), 7.36 (m, 3H), 7.54 (m, 1H), 7.60 (m, 1H), 7.69 (m, 4H), 7.78 (m, 2H), 7.90 (m, 4H), 8.20 (m, 1H), 8.46 (m, 1H), 8.71 (d, J = 7.0 Hz, 1H). LC/MS: method 1, retention time 5.520 min. HRMS (m/z): calcd for $C_{29}H_{25}ClN_2PS^+$ $(M)^+$ 499.1168, found 499.1163.

*(E)-1-(3-(4-Chlorophenyl)allyl)-3-(diphenylphosphorothioyl)-2-methylimidazo[1,2-a]pyridin-1-ium Trifluoroacetate (**21d**).* ^{1}H NMR (400 MHz, DMSO-d_6): δ 1.75 (d, 3H), 5.28 (m, 2H), 6.47 (m, 1H), 6.84 (d, J = 16.0 Hz, 1H), 7.41 (m, 2H), 7.47 (m, 2H), 7.59 (td, J = 7.1, 1.2 Hz, 1H), 7.69 (m, 4H), 7.78 (m, 2H), 7.91 (m, 4H), 8.20 (ddd, J = 9.2, 7.2, 1.2 Hz, 1H), 8.47 (m, 1H), 8.70 (m, 1H). LC/MS: method 1, retention time 5.503 min. HRMS (m/z): calcd for $C_{29}H_{25}ClN_2PS^+$ $(M)^+$ 499.1168, found 499.1166.

*(E)-3-(Diphenylphosphorothioyl)-2-methyl-1-(3-(4-(trifluoromethyl)phenyl)allyl)imidazo[1,2-a]pyridin-1-ium Trifluoroacetate (**21e**).* ^{1}H NMR (400 MHz, DMSO-d_6): δ 1.75 (d, J = 1.4 Hz, 3H), 5.32 (dd, J = 6.7, 0.9 Hz, 2H), 6.62 (dt, J = 16.1, 6.0 Hz, 1H), 6.92 (d, J = 16.0 Hz, 1H), 7.59 (td, J = 7.0, 1.2 Hz, 1H), 7.68 (m, 8H), 7.78 (m, 2H), 7.91 (m, 4H), 8.20 (ddd, J = 8.9, 7.3, 1.2 Hz, 1H), 8.47 (dd, J = 9.2, 1.0 Hz, 1H), 8.71 (m, 1H). LC/MS: method 1, retention time 5.592 min. HRMS (m/z): calcd for $C_{30}H_{25}F_3N_2PS^+$ $(M)^+$ 533.1427, found 533.1426.

*(E)-1-(3-(4-Bromophenyl)allyl)-3-(diphenylphosphorothioyl)-2-methylimidazo[1,2-a]pyridin-1-ium Trifluoroacetate (**21f**).* ^{1}H NMR (400 MHz, DMSO-d_6): δ 1.74 (d, J = 1.4 Hz, 3H), 5.26 (dd, J = 6.1, 1.2 Hz, 2H), 6.47 (m, 1H), 6.81 (d, J = 16.2 Hz, 1H), 7.40 (d, J = 8.6 Hz, 2H), 7.57 (m, 3H), 7.68 (m, 4H), 7.78 (m, 2H), 7.90 (m, 4H), 8.19 (m, 1H), 8.46 (dd, J = 9.2, 1.2 Hz, 1H), 8.70 (dd, J = 6.9, 1.1 Hz, 1H). LC/MS: method 1, retention time 5.555 min. HRMS (m/z): calcd for $C_{29}H_{25}BrN_2PS^+$ $(M)^+$ 543.0660, found 543.0657.

*(E)-1-(3-(3-Bromophenyl)allyl)-3-(diphenylphosphorothioyl)-2-methylimidazo[1,2-a]pyridin-1-ium Trifluoroacetate (**21g**).* ^{1}H NMR (400 MHz, $CDCl_3$): δ 1.79 (d, J = 0.4 Hz, 3H), 5.35 (m, 2H), 6.20 (m, 1H), 6.57 (d, J = 15.1 Hz, 1H), 7.18 (t, J = 7.7 Hz, 1H), 7.26 (m, 2H), 7.40 (m, 1H), 7.47 (t, J = 1.7 Hz, 1H), 7.63 (m, 6H), 7.96 (m, 5H), 8.13 (m, 1H), 8.81 (d, J = 6.8 Hz, 1H). LC/MS: method 1, retention time 5.552 min. HRMS (m/z): calcd for $C_{29}H_{25}BrN_2PS^+$ $(M)^+$ 543.0660, found 543.0662.

*(E)-1-(3-(3-Bromo-4-fluorophenyl)allyl)-3-(diphenylphosphorothioyl)-2-methylimidazo[1,2-a]pyridin-1-ium Trifluoroacetate (**21h**).* ^{1}H NMR (400 MHz, $CDCl_3$): δ 1.79 (d, J = 1.4 Hz, 3H), 5.35 (m, 2H), 6.14 (m, 1H), 6.58 (d, J = 15.8 Hz, 1H), 7.07 (t, J = 8.3 Hz, 1H), 7.27 (m, 2H), 7.53 (dd, J = 6.6, 2.2 Hz, 1H), 7.59 (m, 4H), 7.67 (m, 2H), 7.96 (m, 5H), 8.13 (d, J = 9.2 Hz, 1H), 8.80 (d, J = 6.7 Hz, 1H). LC/MS: method 1, retention time 5.566 min. HRMS (m/z): calcd for $C_{29}H_{24}BrFN_2PS^+$ $(M)^+$ 561.0564, found 561.0565.

*(E)-3-(Diphenylphosphorothioyl)-2-methyl-1-(3-(naphthalen-2-yl)allyl)imidazo[1,2-a]pyridin-1-ium Bromide (**21i**).* LC/MS: method 1, retention time 5.633 min. HRMS (m/z): calcd for $C_{33}H_{28}N_2PS^+$ $(M)^+$ 515.1712, found 515.1706.

*(E)-3-(Diphenylphosphorothioyl)-1-(3-(4-fluorophenyl)allyl)-2-methylimidazo[1,2-a]pyridin-1-ium Trifluoroacetate (**21j**).* LC/MS: method 1, retention time 5.313 min. HRMS (m/z): calcd for $C_{29}H_{25}FN_2PS^+$ $(M)^+$ 483.1466, found 483.1465.

*(E)-3-(Diphenylphosphorothioyl)-2-methyl-1-(3-p-tolylallyl)-imidazo[1,2-a]pyridin-1-ium Bromide (**21k**).* LC/MS: method 1, retention time 5.491 min. HRMS (m/z): calcd for $C_{30}H_{28}N_2PS^+$ $(M)^+$ 479.1712, found 479.1716.

■ ASSOCIATED CONTENT

Ⓢ Supporting Information

Profile of **20e** against 55 other targets and 2D NMR spectra for **13b**. This material is available free of charge via the Internet at http://pubs.acs.org.

■ AUTHOR INFORMATION

Corresponding Author

*Phone: 301-217-9198. Fax: 301-217-5736. E-mail: maruganj@mail.nih.gov. Address: National Center for Advancing Translational Sciences, 9800 Medical Center Drive, Rockville, MD 20850.

Notes

The authors declare no competing financial interest.

■ ACKNOWLEDGMENTS

This research was supported by the Molecular Libraries Initiative of the National Institutes of Health Roadmap for Medical Research and the Intramural Research Programs of the National Institute on Alcohol Abuse and Alcoholism, NIH. We thank Dr. Reinscheid for generously providing the NPSR clone originally used to generate the CHO-NPSR cell line; Sam Michael for assistance in robotic screening; and William Leister, Paul Shinn, Jeremy Smith, Danielle van Leer, and James Bougie for compound management.

■ ABBREVIATIONS USED

NPS, neuropeptide S; NPSR, neuropeptide S receptor; cAMP, cyclic adenosine monophosphate; MAPK, mitogen-activated protein kinase; SAR, structure−activity relationship; qHTS, quantitative high-throughput screening; HTRF, homogeneous time-resolved fluorescence; ERK, extracellular signal-regulated kinase; Tyr, tyrosine; G-protein, guanosine nucleotide-binding protein; ICV, intracerebroventricular; IP, intraperitoneal; mpk, milligrams per kilogram; DAMGO, [D-Ala^2, N-MePhe^4, Gly-ol]-enkephalin.

■ REFERENCES

(1) Holmes, A.; Heilig, M.; Rupniak, N. M. J.; Steckler, T.; Griebel, G. Neuroropeptide systems as novel therapeutic targets for depression and anxiety disorders. *Trends Pharmacol. Sci.* **2003**, *24*, 580−588.

(2) Sato, S.; Shintani, Y.; Miyajima, N.; Yoshimura, K. Novel G protein-coupled receptor protein and DNA thereof. PCT Int. Appl. WO 2002031145 A1 20020418, 2002.

(3) Xu, Y. L.; Reinscheid, R. K.; Huitron-Resendiz, S.; Clark, S. D.; Wang, Z.; Lin, S. H.; Brucher, F. A.; Zeng, J.; Ly, N. K.; Henriksen, S. J.; de Lecea, L.; Civelli, O. Neuropeptide S: A neuropeptide promoting arousal and anxiolytic-like effects. *Neuron* **2004**, *43*, 487−497.

(4) Xu, Y. L.; Gall, C. M.; Jackson, V. R.; Civelli, O.; Reinscheid, R. K. Distribution of neuropeptide S receptor mRNA and neurochemical characteristics of neuropeptide S-expressing neurons in the rat brain. *J. Comp. Neurol.* **2007**, *500*, 84−102.

(5) Reinscheid, R. K.; Xu, Y. L.; Okamura, N.; Zeng, J.; Chung, S.; Pai, R.; Wang, Z.; Civelli, O. Pharmacological characterization of human and murine neuropeptide S receptor variants. *J. Pharmacol. Exp. Ther.* **2005**, *315*, 1338−1345.

(6) Laitinen, T.; Polvi, A.; Rydman, P.; Vendelin, J.; Pulkkinen, V.; Salmikangas, P.; Makela, S.; Rehn, M.; Pirskanen, A.; Rautanen, A.; Zucchelli, M.; Gullstén, H.; Leino, M.; Alenius, H.; Petäys, T.; Haahtela, T.; Laitinen, A.; Laprise, C.; Hudson, T. J.; Laitinen, L. A.; Kere, J. Characterization of a common susceptibility locus for asthma-related traits. *Science* **2004**, *304*, 300−304.

(7) Koob, G. F.; Greenwell, T. N. Neuropeptide S: A novel activating anxiolytic? *Neuron* **2004**, *43*, 441−442.

(8) Beck, B.; Fernette, B.; Stricker-Krongrad, A. Peptide S is a novel potent inhibitor of voluntary and fast-induced food intake in rats. *Biochem. Biophys. Res. Commun.* **2005**, *332*, 859−865.

(9) Cannella, N.; Economidou, D.; Kallupi, M.; Stopponi, S.; Heilig, M.; Massi, M.; Ciccocioppo, R. Persistent increase of alcohol-seeking evoked by neuropeptide S: An effect mediated by the hypothalamic hypocretin system. *Neuropsychopharmacology* **2009**, *34*, 2125−2134.

(10) Smart, D.; Sabido-David, C.; Brough, S. J.; Jewitt, F.; Johns, A.; Porter, R. A.; Jerman, J. C. SB-334867-A: The first selective orexin-1 receptor antagonist. *Br. J. Pharmacol.* **2001**, *132*, 1179−1182.

(11) (a) Pañeda, C.; Huitron-Resendiz, S.; Frago, L. M.; Chowen, J. A.; Picetti, R.; de Lecea, L.; Roberts, A. J. Neuropeptide S reinstates

cocaine-seeking behavior and increases locomotor activity through corticotropin-releasing factor receptor 1 in mice. *J. Neurosci.* **2009**, *29*, 4155−4161. (b) Li, W.; Gao, Y.; Chang, M.; Peng, Y.; Yao, J.; Han, R.; Wang, R. Neuropeptide S inhibits the acquisition and the expression of conditioned place preference to morphine in mice. *Peptides* **2009**, *30*, 234−240.

(12) (a) Guerrini, R.; Salvadori, S.; Rizzi, A.; Regoli, D.; Calo, G. Neurobiology, pharmacology, and medicinal chemistry of neuropeptide S and its receptor. *Med. Res. Rev.* **2010**, *30*, 751−777. (b) Pape, H.-C.; Jüngling, K.; Seidenbecher, T.; Lesting, J.; Reinscheid, R. K. Neuropeptide S: a transmitter system in the brain regulating fear and anxiety. *Neuropharmacology* **2009**, *58*, 29−34. (c) Lei, Z.; Yao, Y.; Li, Y.; Yang, G. *Xumu Yu Shouyi* **2008**, *40*, 97−100. (d) Okamura, N.; Reinscheid, R. K. Neuropeptide S: A novel modulator of stress and arousal. *Stress* **2007**, *10*, 221−226.

(13) (a) Guerrini, R.; Camarda, V.; Trapella, C.; Caló, G.; Rizzi, A.; Ruzza, C.; Fiorini, S.; Marzola, E.; Reinscheid, R. K.; Regoli, D.; Salvadori, S. Further studies at neuropeptide S position 5: discovery of novel neuropeptide S receptor antagonists. *J. Med. Chem.* **2009**, *52*, 4068−4071. (b) Guerrini, R.; Camarda, V.; Trapella, C.; Calò, G.; Rizzi, A.; Ruzza, C.; Fiorini, S.; Marzola, E.; Reinscheid, R. K.; Regoli, D.; Salvadori, S. Synthesis and biological activity of human neuropeptide S analogues modified in position 5: Identification of potent and pure neuropeptide S receptor antagonists. *J. Med. Chem.* **2009**, *52*, 524−529. (c) Camarda, V.; Trapella, C.; Caló, G.; Guerrini, R.; Rizzi, A.; Ruzza, C.; Fiorini, S.; Marzola, E.; Reinscheid, R. K.; Regoli, D.; Salvadori, S. Synthesis and biological activity of human neuropeptide S analogues modified in position 2. *J. Med. Chem.* **2008**, *51*, 655−658.

(14) Fukatsu, K.; Nakayama, Y.; Tarui, N.; Mori, M.; Matsumoto, H.; Kurasawa, O.; Banno, H. Bicyclic piperazine compound and use thereof. PCT Int. Appl. WO 2005021555 A1 20050310, 2005.

(15) Okamura, N.; Habay, S. A.; Zeng, J.; Chamberlin, A. R.; Reinscheid, R. K. Synthesis and pharmacological in vitro and in vivo profile of 3-oxo-1,1-diphenyl-tetrahydro-oxazolo[3,4-a]pyrazine-7-carboxylic acid 4-fluoro-benzylamide (SHA 68), a selective antagonist of the neuropeptide S receptor. *J. Pharmacol. Exp. Ther.* **2008**, *325*, 893−901.

(16) Trapella, C.; Pela, M.; Del Zoppo, L.; Calo, G.; Camarda, V.; Ruzza, C.; Cavazzini, A.; Costa, V.; Bertolasi, V.; Reinscheid, R. K.; Salvadori, S.; Guerrini, R. Synthesis and separation of the enantiomers of the neuropeptide S receptor antagonist (9*R*/*S*)-3-oxo-1,1-diphenyl-tetrahydro-oxazolo[3,4-*a*]pyrazine-7-carboxylic acid 4-fluoro-benzylamide (SHA 68). *J. Med. Chem.* **2011**, *54*, 2738−2744.

(17) Melamed, J. Y.; Zartman, A. E.; Kett, N. R.; Gotter, A. L.; Uebele, V. N.; Reiss, D. R.; Condra, C. L.; Fandozzi, C.; Lubbers, L. S.; Rowe, B. A.; McGaughey, G. B.; Henault, M.; Stocco, R.; Renger, J. J.; Hartman, G. D.; Bilodeau, M. T.; Trotter, B. W. Synthesis and evaluation of a new series of neuropeptide S receptor antagonists. *Bioorg. Med. Chem. Lett.* **2010**, *20*, 4700−4703.

(18) Trotter, B. W.; Nanda, K. K.; Manley, P. J.; Uebele, V. N.; Condra, C. L.; Gotter, A. L.; Menzel, K.; Henault, M.; Stocco, R.; Renger, J. J.; Hartman, G. D.; Bilodeau, M. T. Tricyclic imidazole antagonists of the neuropeptide S receptor. *Bioorg. Med. Chem. Lett.* **2010**, *20*, 4704−4708.

(19) Micheli, F.; Di Fabio, R.; Giacometti, A.; Roth, A.; Moro, E.; Merlo, G.; Paio, A.; Merlo-Pich, E.; Tomelleri, S.; Tonelli, F.; Zarantonello, P.; Zonzini, L.; Capelli, A. M. Synthesis and pharmacological characterization of 5-phenyl-2-[2-(1-piperidinylcarbonyl)phenyl]-2,3-dihydro-1*H*-pyrrolo[1,2-*c*]imidazol-1-ones: A new class of neuropeptide S antagonists. *Bioorg. Med. Chem. Lett.* **2010**, *20*, 7308−7311.

(20) Fretz, H.; Gatfield, J.; Isler, M.; Kimmerlin, T.; Koberstein, R.; Lyothier, I.; Monnier, L.; Pothier, J.; Valdenaire, A. Indanone and indandione derivatives and heterocyclic analogs. PCT Int. Appl. WO 2013068785 A1 20130516, 2013.

(21) McCoy, J. G.; Marugan, J. J.; Liu, K.; Zheng, W.; Southall, N.; Heilig, M.; Austin, C. A. Selective Modulation of Gq/Gs pathways by Naphtho Pyrano Pyrimidines as antagonists of the Neuropeptide S Receptor. *ACS Chem. Neurosci.* **2010**, *1*, 559−574.

(22) Dal Ben, D.; Antonini, I.; Buccioni, M.; Lambertucci, C.; Marucci, G.; Thomas, A.; Volpini, R.; Cristalli, G. Neuropeptide S receptor: Recent updates on nonpeptide antagonist discovery. *ChemMedChem* **2011**, *6*, 1163−1171.

(23) qHTS Assay for Antagonists of the Neuropeptide S Receptor: cAMP Signal Transduction. Pub Chem AID 1461. http://pubchem.ncbi.nlm.nih.gov/assay/assay.cgi?aid=1461&loc=ea_ras (accessed Nov 5, 2013).

(24) Available commercially at Enamine, cat. no. T0504-5950.

(25) Bakherad, M.; Nasr-Isfahani, H.; Keivanloo, A.; Bakherad, M.; Doostmohammadi, N. Pd−Cu catalyzed heterocyclization during Sonogashira coupling: Synthesis of 2-benzylimidazo[1,2-*a*]pyridine. *Tetrahedron Lett.* **2008**, *49*, 3819−3822.

(26) (a) Tolmachev, A. A.; Yurchenko, A. A.; Kozlov, E. S.; Merkulov, A. S.; Semenova, M. G.; Pinchuk, A. M. Phosphorylated Imidazo[1,2-*a*] pyridines. *Heteroat. Chem.* **1995**, *5*, 419−432. (b) Tolmachev, A. A.; Yurchenko, A. A.; Kozlov, E. S. Phosphorylation of 2-methylimidazo[1,2-*a*]pyridine. Rare cases of nitrogen-atom alkylation of a phosphine and phosphonite. *J. Gen. Chem. USSR (Engl. Transl.).* **1992**, *62*, 1369−1371.

(27) Romanenko, V. D.; Tovstenko, V. I.; Markovski, L. N. Applications of iodotrimethylsilane for the synthesis of iodophosphines, iodophosphoranes, and iodomethylphosphine oxides. *Synthesis* **1980**, 823−825.

(28) The alkylation proceeds at the N1 position as expected from similar compounds described earlier in the literature (ref 25). The regiochemistry of alkylation was also proved by the interpretation of COSY, HMQC, HMBC, and NOESY spectra of **13b** (see the Supporting Information). The masses of the fragments acquired via mass spectrometry of **13a**, **13b**, and **20e** also support alkylation at N1 of the imidazopyridine.

(29) Benincori, T.; Piccolo, O.; Rizzo, S.; Sannicolò, F. 3,3′-Bis(diphenylphosphino)-1,1′-disubstituted-2,2′-biindoles: Easily accessible, electron-rich, chiral diphosphine ligands for homogeneous enantioselective hydrogenation of oxoesters. *J. Org. Chem.* **2000**, *65*, 8340−8347.

(30) Krasovskiy, A.; Knochel, P. A LiCl-mediated Br/Mg exchange reaction for the preparation of functionalized aryl- and heteroarylmagnesium compounds from organic bromides. *Angew. Chem., Int. Ed.* **2003**, *43*, 3333−3336.

(31) The IC_{50} values reported in Tables 1−3 were calculated from assays that were performed in 1536-well format. We observed slightly weaker potencies while testing in a 386-well format. Also, it appeared that the chemical series discussed in this communication, as exemplified by **7** and **20e**, had enhanced potencies towards inhibition of ERK phosphorylation in the 386-well format. This observation has been emphasized in a separate communication.[32]

(32) Fedeli, A.; Braconi, S.; Economidou, D.; Cannela, N.; Kallupi, M.; Guerrini, R.; Calò, G.; Cifani, C.; Massi, M.; Ciccocioppo, R. The paraventricular nucleus of the hypothalamus is a neuroanatomical substrate for the inhibition of palatable food intake by neuropeptide S. *Eur. J. Neurosci.* **2009**, *30*, 1594−1602.

(33) Di, L.; Rong, H.; Feng, B. Demystifying brain penetration in central nervous system drug discovery. *J. Med. Chem.* **2013**, *56*, 2−12.

(34) Thorsell, A.; Tapocik, J. D.; Liu, K.; Zook, M.; Bell, L.; Flanigan, M.; Patnaik, S.; Marugan, J.; Damadzic, R.; Dehdashti, S.; Schwandt, M. L.; Southall, N.; Austin, C. A.; Eskay, R.; Ciccocioppo, R.; Zheng, W.; Heilig, M. A novel brain penetrant NPS receptor antagonist, NCGC00185684, blocks alcohol-induced ERK-phosphorylation in the central amygdala and decreases operant alcohol self-administration in rats. *J. Neurosci.* **2013**, *33*, 10132−10142.

(35) Calculated properties for **20e** as per ChemBioDraw Ultra 12.0: ClogP 3.33, tPSA 6.25. Measured solubility of **20e** in PBS: kinetic solubility >150 μM, equilibrium solubility ∼45 μM.